

Biofouling

The Journal of Bioadhesion and Biofilm Research

ISSN: 0892-7014 (Print) 1029-2454 (Online) Journal homepage: <http://www.tandfonline.com/loi/gbif20>

Engineered antifouling microtopographies: kinetic analysis of the attachment of zoospores of the green alga *Ulva* to silicone elastomers

Scott P. Cooper , John A. Finlay , Gemma Cone , Maureen E. Callow , James A. Callow & Anthony B. Brennan

To cite this article: Scott P. Cooper , John A. Finlay , Gemma Cone , Maureen E. Callow , James A. Callow & Anthony B. Brennan (2011) Engineered antifouling microtopographies: kinetic analysis of the attachment of zoospores of the green alga *Ulva* to silicone elastomers, *Biofouling*, 27:8, 881-892, DOI: [10.1080/08927014.2011.611305](https://doi.org/10.1080/08927014.2011.611305)

To link to this article: <https://doi.org/10.1080/08927014.2011.611305>

 View supplementary material 

 Published online: 01 Sep 2011.

 Submit your article to this journal 

 Article views: 800

 Citing articles: 33 View citing articles 

Engineered antifouling microtopographies: kinetic analysis of the attachment of zoospores of the green alga *Ulva* to silicone elastomers

Scott P. Cooper^a, John A. Finlay^b, Gemma Cone^b, Maureen E. Callow^b, James A. Callow^b and Anthony B. Brennan^{a*}

^aDepartment of Materials Science and Engineering, University of Florida, Gainesville, Florida, USA; ^bSchool of Biosciences, University of Birmingham, Birmingham, UK

(Received 20 April 2011; final version received 3 August 2011)

Microtopography has been demonstrated as an effective deterrent to biofouling. The majority of published studies are fixed-time assays that raise questions regarding the kinetics of the attachment process. This study investigated the time-dependent attachment density of zoospores of *Ulva*, in a laboratory assay, on a micropatterned and smooth silicone elastomer. The attachment density of zoospores was reduced on average 70–80% by the microtopography relative to smooth surfaces over a 4 h exposure. Mapping the zoospore locations on the topography revealed that they settled preferentially in specific, recessed areas of the pattern. The kinetic data fit, with high correlation ($r^2 > 0.9$), models commonly used to describe the adhesion of bacteria to surfaces. The grouping of spores on the microtopography indicated that the pattern inhibited the ability of attached spores to recruit neighbors. This study demonstrates that the antifouling mechanism of topographies may involve disruption of the cooperative effects exhibited by fouling organisms such as *Ulva*.

Keywords: biofouling; antifouling; algae; topography; roughness; kinetics; *Ulva*

Introduction

Marine biofouling is a costly, complex and environmentally harmful phenomenon. Biofouling on ship hulls increases fuel consumption and necessitates regular hull cleaning. A recent estimate by Schultz et al. (2011) put the cost of biofouling at \$1 billion over 15 years for the US Navy Arleigh Burke (DDG) class of destroyers. Hull fouling is also a primary vector for the introduction of invasive species (Drake and Lodge 2007; Piola et al. 2009). The majority of antifouling (AF) coatings contain biocides (Finnie and Williams 2010; Thomas and Brooks 2010), but environmental issues have increased interest in the development of non-toxic AF coatings, which encompass a wide range of technologies (eg McMaster et al. 2009; Tasso et al. 2009; Bressy et al. 2010; Kristensen et al. 2010; Sommer et al. 2010).

One environmentally-friendly approach is to use microtopography on a surface to deter biofouling. Many AF topographies are inspired by marine organisms that naturally exhibit low fouling such as crabs, mussels and sharks (Scardino et al. 2009; Magin et al. 2010a; Scardino and de Nys 2011). Our group has developed an AF topography inspired by the skin of a shark, called Sharklet. This topography has been shown to inhibit attachment of zoospores of *Ulva*

(Carman et al. 2006; Schumacher et al. 2007a, 2007b, 2008; Long et al. 2010b); cyprids of *Balanus amphitrite* (Schumacher et al. 2007a); and cells of the bacteria *Cobetia marina* (Magin et al. 2010b) and *Staphylococcus aureus* (Chung et al. 2007). In a kinetic study, the Sharklet pattern inhibited biofilm formation of non-motile *S. aureus* cells for up to 21 days (Chung et al. 2007). However, no kinetic analysis of attachment rates for the motile zoospores of *Ulva*, which is a common fouling alga in the marine environment, has been performed on microtopographically patterned polydimethylsiloxane elastomers (PDMS_e).

The purpose of this study was to investigate the initial attachment kinetics of the zoospores of *Ulva* on Sharklet patterned and smooth PDMS_e, which should provide insight into how Sharklet topography functions as an AF surface. Observations of zoospores of *Ulva* reveal that the cells do not necessarily adhere to a surface on first contact. Rather, through temporary and therefore reversible contacts (previously referred to as ‘first kiss’ adhesion [Callow and Callow 2002]), they ‘probe’ a surface numerous times before committing themselves to a permanent, irreversible adhesion involving the secretion of an adhesive pad (Callow et al. 1997; Heydt et al. 2009). The ‘first kiss’ phase of adhesion allows spores to respond to a range of surface

*Corresponding author. Email: abrennan@mse.ufl.edu

cues or features, potentially resulting in preferential attachment to specific locations rather than being randomly distributed over the surface. For example, spores may attach in close vicinity to previously attached spores, ie gregarious attachment (Callow et al. 1997). In the context of the present paper, attachment of single spores to specific topographical elements has been observed on Sharklet over a 45 min assay (Long et al. 2010a). Yet, it is unknown whether preferential attachment occurs only during the early stages of fouling or whether spores become less selective with time, leading to the topography becoming a less effective fouling deterrent. In the present study, the distributions of spores, which are attached either as individuals or in groups, on the topography are mapped *vs* time in order to address this question.

The experiment was also designed to test whether the spores would ‘choose’ to settle on a smooth surface rather than the Sharklet pattern if given a choice. Test slides (19.4 cm²) were prepared with various areal coverage of the Sharklet pattern (see Figure 1A–C) to examine the issue of ‘choice’ by the zoospores. Slides with partial patterning were made by covering a 6.5 cm² area with the Sharklet pattern (see Figure 1B). The ability of the spore to preferentially ‘choose’ a surface was tested by comparing the attachment kinetics among different sample geometries (Figure 1).

Materials and methods

Sample preparation

All test surfaces were fabricated with polydimethylsiloxane elastomer (PDMS_e, Dow Corning Silastic[®])

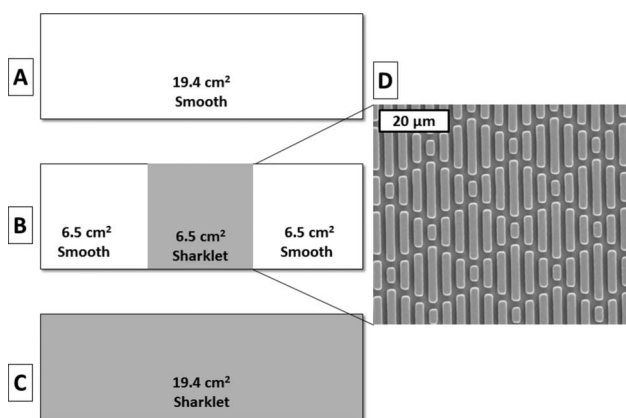


Figure 1. Schematic of sample arrangements on 2.54 cm × 7.62 cm glass slides. (A) 19.4 cm² area of smooth PDMS_e coating on glass slide; (B) 6.5 cm² area of Sharklet micropatterned (+2.5SK2 × 2) PDMS_e on glass slide adjacent to two 6.5 cm² areas of smooth PDMS_e; (C) 19.4 cm² area Sharklet micropatterned (+2.5SK2 × 2) PDMS_e on glass slide; (D) SEM image of +2.5SK2 × 2 topography.

T2). The PDMS_e surfaces were attached to glass slides 2.54 cm × 7.62 cm (total area 19.4 cm²) for all experiments. All PDMS_e surfaces were prepared by mixing T2 base and curing agent at a 10:1 weight ratio for 5 min. The T2 was degassed for 30 min under vacuum and cured for 24 h at ≈22°C.

To create smooth surfaces, T2 was cast against glass with a vapor-deposited coating of hexamethyldisilazane (HMDS). PDMS_e surfaces with the Sharklet topography were made by casting against etched silicon wafers. The silicon wafer molds were prepared by photolithography and deep reactive ion etching as previously described (Long et al. 2010a). Silicon wafers were vapor deposited with HMDS to prevent adhesion of cured PDMS_e. All samples were rinsed with 95% ethanol for approximately 10 s and blown with nitrogen prior to shipping. As noted previously (Long et al. 2010b), the topography on the Sharklet samples (eg +2.8SK2 × 2) is designated as:

(Feature height in µm) SK (Feature width in µm)
× (Feature spacing in µm)

Attachment assay for zoospores

Two kinetic attachment assays were performed on different dates. Assay 1 was performed in October 2009 and tested sample arrangements A and B in Figure 1. Assay 2 was performed in April 2010 and tested sample arrangements A, B, and C in Figure 1.

Samples were shipped dry to the University of Birmingham. Each test surface was placed in an individual compartment (83 × 30 mm) of a Quadriperm dish (Greiner Bio-one Ltd). Test surfaces were immersed in 0.22 µm filtered artificial seawater (ASW) (Tropic Marin, Aquarientechnik GmbH) for 24 h prior to the experiment. Any air visibly trapped in the features was dispersed using a stream of seawater from a pipette.

Zoospores were released from fertile tips of mature plants of *Ulva linza* into 0.22 µm filtered artificial seawater (ASW; ‘Tropic Marin’, Aquarientechnik GmbH), as described in Schumacher et al. (2007b). After filtering through three layers of nylon plankton net of decreasing pore size (100, 35 and 20 µm) into a glass beaker, the spore suspension was concentrated by plunging the beaker into crushed ice (spores rapidly swim towards the bottom of the beaker). The concentrated suspension of spores was pipetted into a clean beaker and the procedure was repeated. The spore suspension was diluted with filtered ASW to give an absorbance of 0.15 at 660nm, equivalent to 1 × 10⁶ spores ml⁻¹. The suspension was kept on a magnetic stirrer to ensure the spores did not attach to the container. Ten ml of the spore suspension were added

to each compartment of the dishes containing the test slides. The dishes were incubated at room temperature ($\approx 20^\circ\text{C}$) in darkness for periods up to 4 h. Three replicates (slides) were analyzed at each time point. At each time point the slides were washed to remove unattached (ie still swimming) spores by passing the slides 10 times through a beaker of ASW. Slides were subsequently fixed with 2.5% glutaraldehyde in ASW for 15 min before washing sequentially in ASW, 50% ASW and distilled water, then dried.

The density of zoospores attached to the surface was determined using a Zeiss Kontron 3000 image analysis system attached to a Zeiss Axioplan fluorescence microscope as described in Callow et al. (2002). Spores were visualized by autofluorescence of chlorophyll. Spore densities on slides A and C (Figure 1) were counted in a line across the middle of the slide at 1–2 mm intervals, 30 counts per replicate slide (each 0.17 mm^2). Spores in the 6.5 cm^2 smooth areas adjacent to the topography (slide B, Figure 1) were counted in the same way with 15 fields of view on either side of the Sharklet pattern. Counts on the 6.5 cm^2 Sharklet pattern (slide B, Figure 1) were taken with 15 counts horizontal and 15 counts vertical to the approximate midpoint of the patterned area.

Zoospore mapping and grouping distribution

Attachment maps were created as described previously (Long 2009; Long et al. 2010a) to show the preferred attachment locations of zoospores on the topography. Thirty-six transmitted light micrographs ($186\ \mu\text{m} \times 138\ \mu\text{m}$) of the Sharklet pattern (6.5 cm^2) per time point were used from the October 2009 assay for attachment maps and spore grouping analysis. These images were selected because they contained spores. The center of each spore was identified using Image J (US National Institute of Health) by overlaying the spore body with a black ellipse and subsequently using the threshold and particle measurement functions of the software. The coordinates for the center of the spore were transformed to correct for the orientation of the topography in the image. The resulting coordinates of each spore location were graphed on a unit cell of the topography and the spore location was individually checked against the original image for accuracy. The coordinates for the spores were processed with a Kernel smoothing algorithm in Matlab (The MathWorks, Inc). This algorithm creates a smooth probability density function from a two-dimensional histogram. Warm colors on the map indicate a high probability of attachment at the given time point. During the mapping process, each individual zoospore was identified as having attached in a group of 1, 2, 3, or >3 spores. The group size was

determined by the number of spores visually touching in the micrographs. These data were used in the analysis of spore grouping. Attachment maps for groups of 2, 3, or >3 spores represent the location of each individual spore within the group.

Statistical analysis

Attachment densities were counted as the average over 90 fields of view (3 replicates, 30 fields of view per replicate). 95% confidence intervals for reduction of attachment density were calculated by an arcsine transformation. SigmaStat 3.1 (Systat Software, Inc.) was used to perform analysis of variance (ANOVA), Tukey, and chi-squared tests. Fitting of the kinetic response was performed by a least squares fit algorithm in Matlab with the EzyFit package (Université Paris-Sud).

Results

Kinetic attachment assays

Zoospores attached at a higher density on smooth surfaces than on Sharklet surfaces for every time point during the 4-h experiment (Figure 2). The attachment response was the same for the smooth surface regardless of whether it completely covered the slide or was adjacent to the Sharklet topography. Spores were inhibited by the Sharklet topography regardless of the areal coverage on the test slide (6.5 cm^2 or 19.4 cm^2).

This kinetic attachment assay was conducted twice to ensure reproducibility (Figure 2 and Supplementary Information Figure S1 [Supplementary material is available *via* a multimedia link on the online article webpage]). The zoospores responded to the surfaces in the same manner for both tests. The first assay,

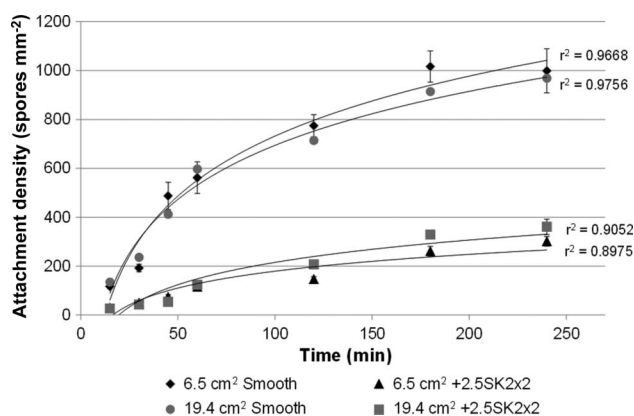


Figure 2. Kinetic response of zoospores of *Ulva* to smooth and Sharklet PDMSe surfaces. Error bars indicate 95% confidence intervals. Correlation coefficients are for the fit of Equation (1) to the attachment data.

performed in October 2009, had lower zoospore attachment densities than the assay performed in April 2010. However, previous studies show that there is

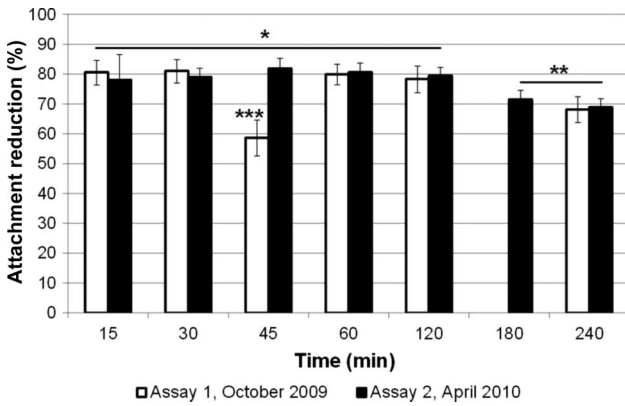


Figure 3. Reduction in attachment of zoospores on Sharklet microtopography versus smooth PDMS_e (6.5 cm² areas). Results are shown for two assays. Groups indicated by asterisks were shown to be similar ($p < 0.05$) by a Tukey test. Error bars indicate 95% confidence intervals.

natural variability in the absolute numbers of attached spores from one experiment to another (Callow et al. 1997).

Despite the variability in absolute settled spore density, a one-way ANOVA ($df = 12$, $F = 14.065$, $p < 0.001$) with a Tukey test ($p < 0.05$) showed that the reduction in zoospore density on the Sharklet surfaces is constant at 80% for up to 2 h (Figure 3). The attachment reduction is lower at 70% for the 180 and 240 min time points. These results were consistent between the two assays with the exception of assay 1 at 45 min. The percentage reduction in spore density is comparable to previous studies (Carman et al. 2006; Schumacher et al. 2007a, 2007b, 2008; Long et al. 2010b) in which the positive SK2 \times 2 surface reduced attachment of spores by 63-86% over a 45 min assay.

Mapping spore attachment

Mapping the attachment of zoospores on the Sharklet topography qualitatively illustrates the kinetic fouling

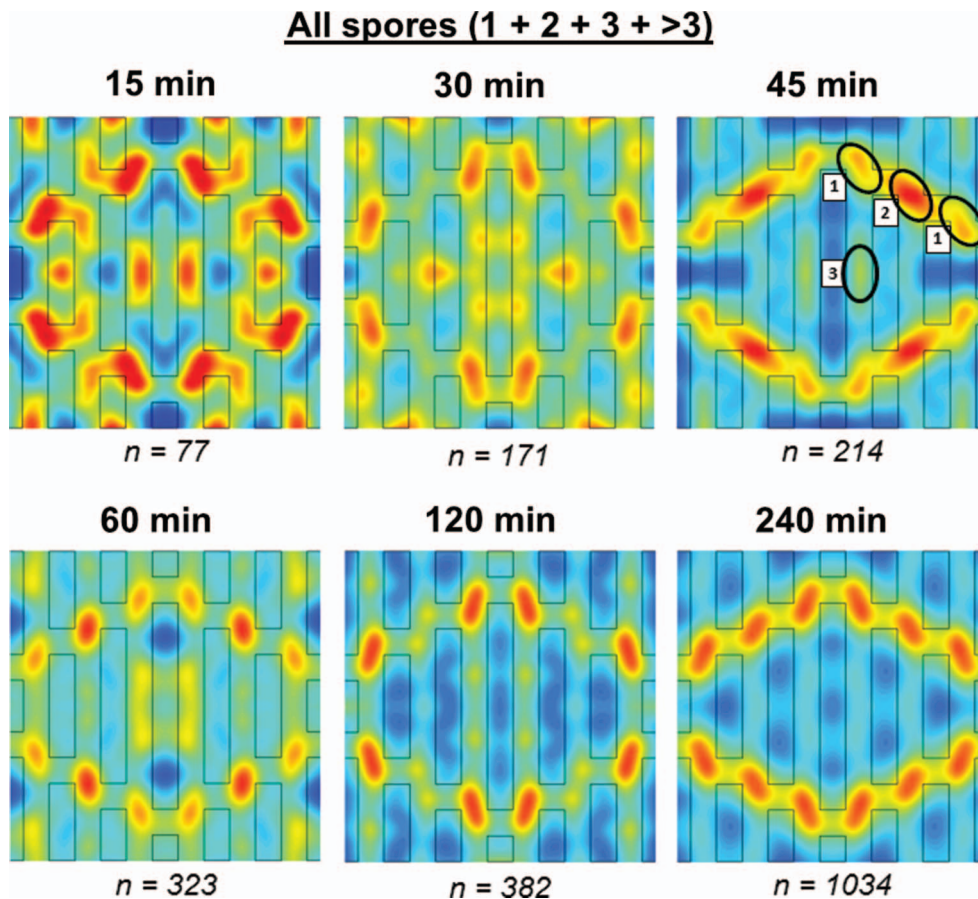


Figure 4. Maps of all zoospores attached to the Sharklet topography during the kinetic study. The number of spores used to create each map is given by n . The map at 45 min indicates the sites of high preferential settlement (1, 2, and 3) that were originally described by Long et al. (2010a). Warm colors indicate high attachment density for that time point. Colors cannot be compared between time points.

process. The maps for all spores attached to the Sharklet topography (Figure 4) reveal that zoospores prefer to attach in the depressed areas between features, rather than on top of them. The spores exhibit a higher selectivity for three particular sites on the Sharklet topography, as noted in a previous publication (Long et al. 2010a). Two of these sites are located at the ends of the features and a third site adjacent to midpoint of the longest feature. Fifty percent of the spores attached in these three sites, which account for only 31% of the total surface. The spores' selectivity appears to favor site 1 relative to site 3 for all times other than 15 min. There also appears to be a decreasing selectivity for site 3 beyond 45 min. Site 1 and site 2 appear to be equivalent in terms of spore selectivity (Figures 4 and S2).

Breaking down the attachment maps for all spores (Figure 4) into substituent groups (Figures 5–8) provided additional insight. Most of the spores attach to the Sharklet topography as single organisms. As a result, the attachment map for single spores (Figure 5) most closely represents the behavior of all spores attaching to the surface. The preference for attaching

at the edge of the diamond pattern is maintained as the size of the settlement group increases to two and three spores (Figures 6, 7). It also appears that as the size of the group increases, the zone of attachment spreads out from the preferential sites observed for single spores. This indicates that additional spores attach on the surface next to a spore that has already settled. Large groups (>3 spores) were not as selective, especially after 120 min (Figure 8). Large rafts of cells were occasionally seen on the surface at these later times (Supplementary Information Figure S5 [Supplementary material is available *via* a multimedia link on the online article webpage]) which reflects the lack of preference in the settlement maps at these time points.

Spore grouping

The attachment of spores of *Ulva* on smooth surfaces shows the characteristics of 'gregariousness', ie depending on the initial spore density, the attachment of one spore appears to promote the attachment of additional spores in the same vicinity resulting in groups attached to the surface (Callow et al. 1997). The

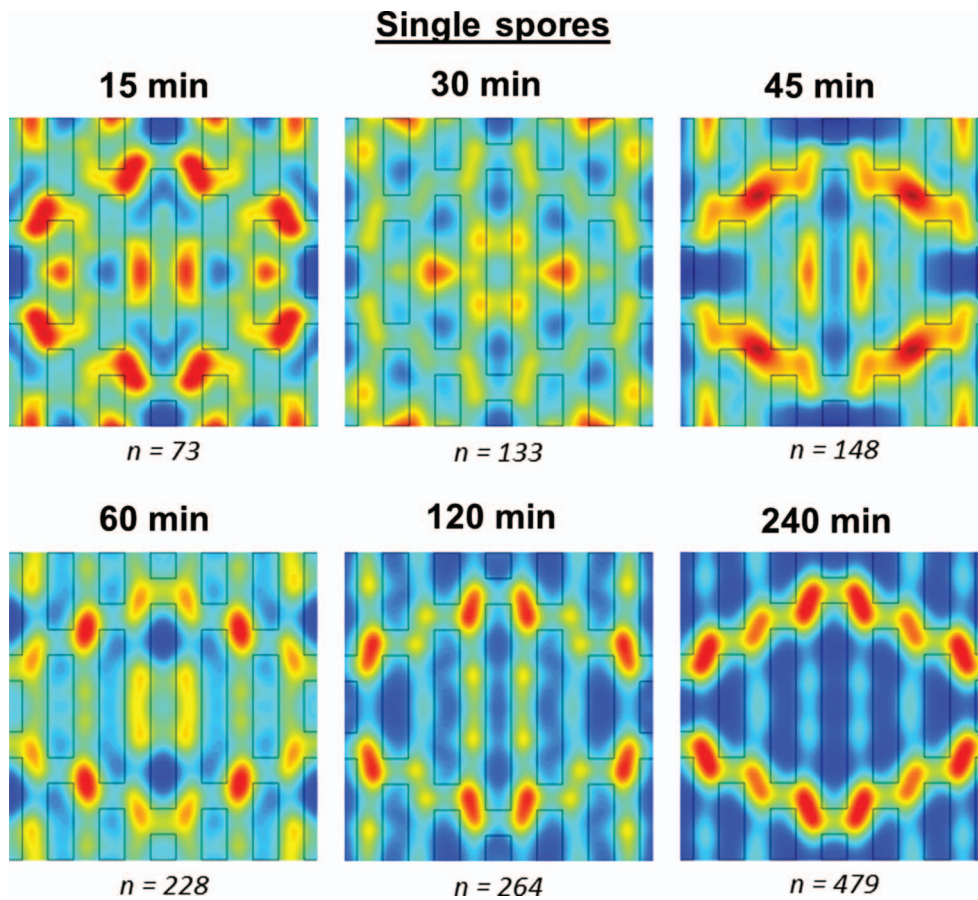


Figure 5. Settlement maps of individual spores on the Sharklet topography. Colors cannot be compared between time points.

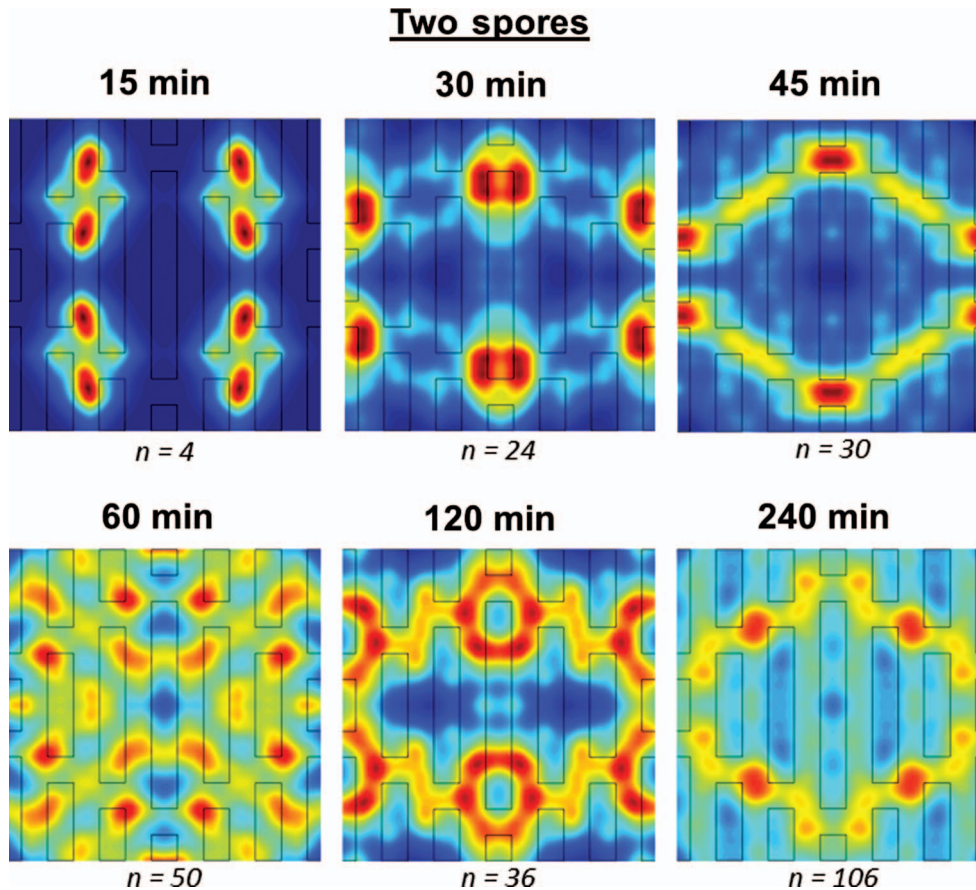


Figure 6. Settlement maps of spores in groups of 2 on the Sharklet topography. Sharp color contrast at early time points arises from low numbers of spores observed on the surface ($n < \sim 50$ spores). Colors cannot be compared between time points.

grouping of spores was compared between Sharklet and smooth surfaces to test whether the topography influenced gregariousness (Figure 9). The Sharklet topography inhibited the ability of spores to form groups of >3 spores. Chi-squared tests revealed that the distributions of spore groups was statistically different between Sharklet and smooth surface at both early (Figure 9A, $\chi^2=371$, $df=3$, $p < 0.001$) and late (Figure 9B, $\chi^2=1143$, $df=3$, $p < 0.001$) time points. Seven percent of spores attached on smooth PDMS as single spores after 240 min compared to 46% of the on the Sharklet microtopography (Figure 9B).

To ensure that the results of this analysis were not caused by a lower density of spores on the Sharklet surface, the spore density after 30 min on smooth (236 spores mm^{-2}) and 120 min on Sharklet (207 spores mm^{-2}) were chosen to compare grouping at approximately the same spore density. The distribution of spore groupings was significantly different for the two surfaces (Figure 9C, $\chi^2=446$, $df=3$, $p < 0.001$). Sixty-nine percent of the spores attached as single cells on the Sharklet topography compared to only 14% on

the smooth surface. Chi-squared tests confirmed that the distributions of spore groupings are statistically different ($p < 0.001$) for Sharklet and smooth (Figure 9A–C).

Discussion

The kinetics of spore attachment on smooth surfaces over a 4 h period revealed an approximately linear rate over the first 60 min, but thereafter the attachment rate progressively decreased. Similar kinetics were reported by Callow et al. (1997) and were ascribed to reduced competence of the zoospore population to attach with time under the assay conditions (ie within a population of ‘wild’ spores, there is a range of propensity for settlement so that with time the population of spores in the assay becomes biased towards those with reduced propensity to settle). In the context of these experiments, two other causes of progressively reduced attachment rates may be operating beyond reduced competence. First, it is likely that with time the surface became progressively conditioned by organic materials either present in the water in which the spores were released, or

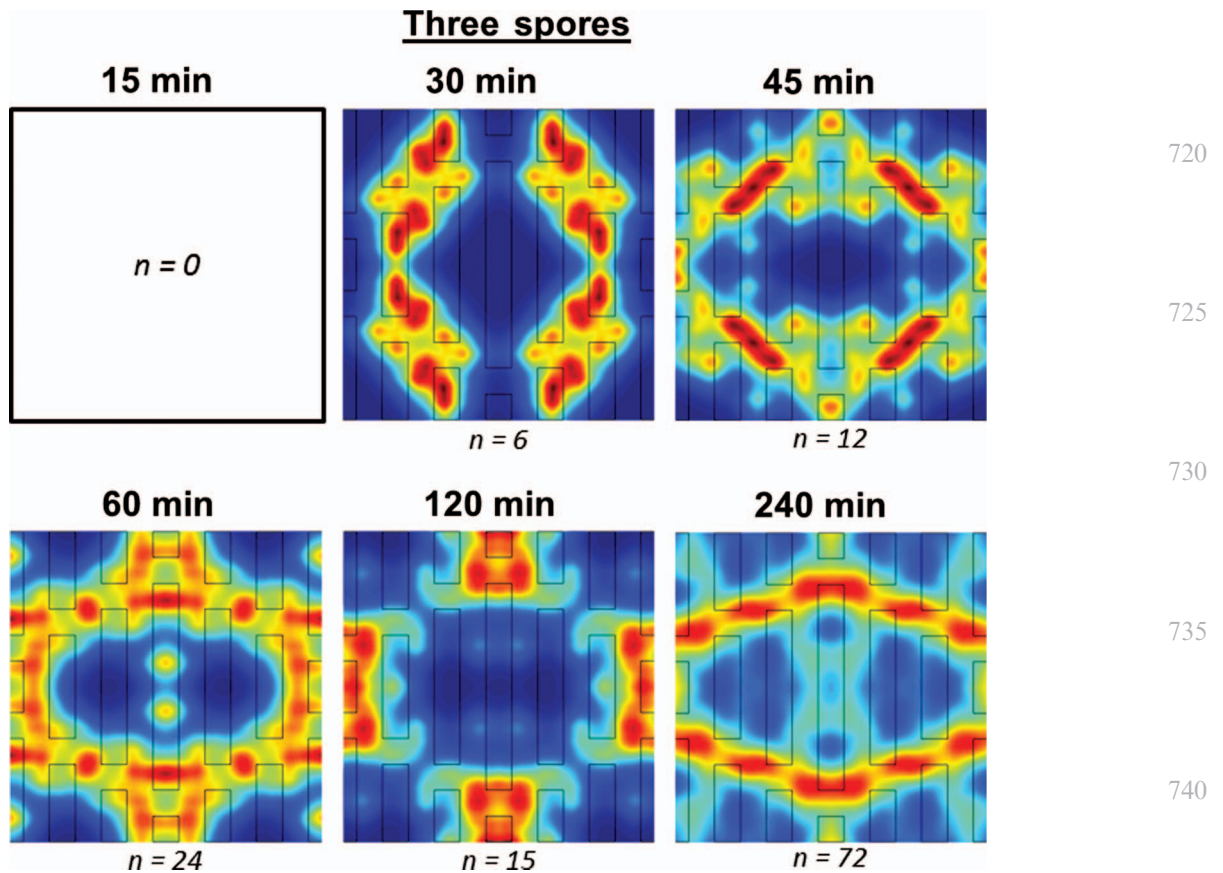


Figure 7. Settlement maps of spores in groups of 3 on the Sharklet topography. No groups of 3 spores were observed after 15 min. Sharp color contrast on some images arises from low numbers of spores observed on the surface ($n < \sim 50$ spores). Colors cannot be compared between time points.

were secreted by the swimming spores. Such conditioning materials could make surfaces less attractive for attachment. Second, the number of swimming spores in solution was reduced over time by attachment to both the test surfaces and especially to the exposed surface of the container in which the test slides were immersed.

The spore attachment density on Sharklet topographies was nearly linear with time and was significantly lower at each time point compared to smooth PDMS_e (70–80% reduction). These results are consistent with previous assays (Carman et al. 2006; Schumacher et al. 2007a, 2007b, 2008; Long et al. 2010b) in which the microtopography reduced attachment densities from 63 to 86% over 45 min.

Mapping the spore attachment sites on the Sharklet microtopography showed that the zoospores preferentially attached in the recessed areas. This is consistent with previous results showing that spores attach preferentially in the recessed channels of PDMS_e patterned surfaces (Callow et al. 2002), specifically at the long ends of the features (Long et al. 2010a). The maps generated in this study capture the attachment at

various time points and also categorize the spores as individuals or part of a group of spores. This was done to identify any cooperative behavior. It appears from the maps that attachment of single spores occurs at preferential sites along the edge of the diamond pattern, with attachment becoming more diffuse along the edge as the size of the group increases. This indicates that additional spores settled adjacent to the first spore during the initial colonization of the surface. It is worth noting that the results of mapping all spores (Figure 4) represent a weighted-average map for spore groups of 1, 2, 3 and >3 cells. The attachment maps for all cells most closely resemble the map for single spores because spores predominantly attach as individuals (Supplementary Information Figure S3 [Supplementary material is available *via* a multimedia link on the online article webpage]).

The kinetic attachment curve can be fitted to the asymptotic exponential function in Equation (1) to provide a quantitative measure of the rate of adhesion. This function was used to describe attachment kinetics of bacteria to surfaces (Dabros and van de Ven 1982;

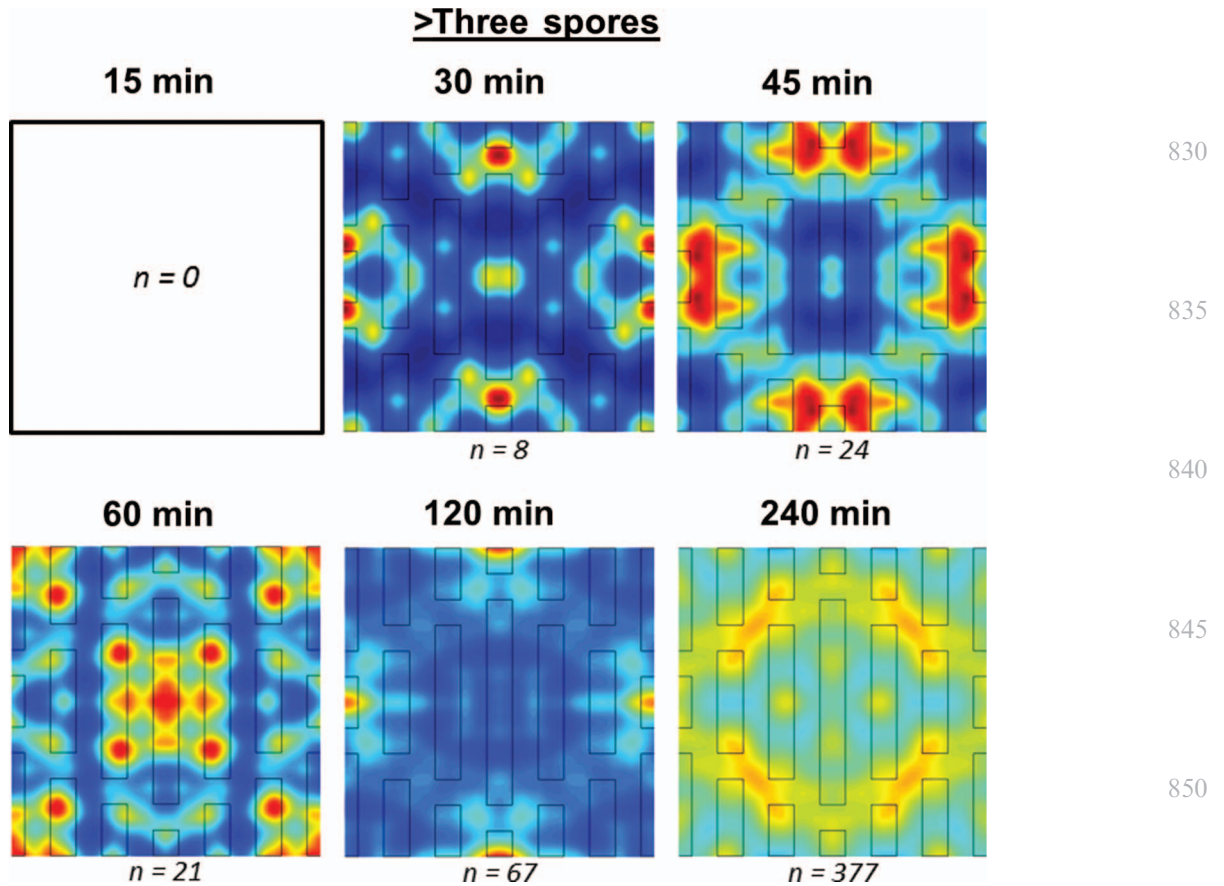
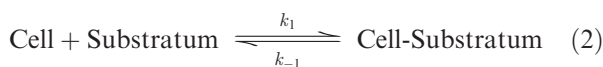


Figure 8. Settlement maps of spores in groups of >3 on the Sharklet topography. No groups of >3 spores were observed after 15 min. Sharp color contrast on some images arises from low numbers of spores observed on the surface ($n < \sim 50$ spores). Colors cannot be compared between time points.

Cowan et al. 1986; Pratt-Terpstra et al. 1988; Sjollem et al. 1989; Busscher et al. 1990):

$$A(t) = A_e(1 - e^{-\beta t}) \quad (1)$$

where $A(t)$ is the number of attached organisms at time t , A_e is the equilibrium density of attached cells, and β is a characteristic time constant. This equation describes the reversible process:



in which k_1 and k_{-1} are the rates of attachment and detachment from the surface, respectively. In the case of *Ulva*, experimental observations of a reversible ‘first kiss’ contact with the surface warrant a model such as that in Equation (2) (Callow et al. 1997). Since these experiments were not performed *in situ*, a direct measure of the adsorption (k_1) and desorption (k_{-1}) cannot be obtained. Equation 1 is fit to the data as an estimation of the kinetic response. A least-squares fit of

this equation provides values for β . Using this time characteristic time constant, the initial flux of spores at the surface can be approximated by the quantity J_o :

$$J_o = A_e \times \beta \quad (3)$$

in which J_o has equivalent units of flux (spores $\text{mm}^{-2} \text{min}^{-1}$).

Fitting Equation (1) to the kinetic data show that the characteristic time constant (β) is distinctly lower on Sharklet surfaces (1.9–3.4 min^{-1}) than on smooth surfaces (9.2–11 min^{-1}) (Table 1). The projected flux, J_o , offers a more physically intuitive sense of the early-stage response of the spores to the surface. J_o for Sharklet was consistently lower (1.3–2.0 spores $\text{mm}^{-2} \text{min}^{-1}$) than J_o for smooth surfaces (6.9–11.5 spores $\text{mm}^{-2} \text{min}^{-1}$). The value of J_o was $\sim 80\%$ lower on Sharklet than on smooth surfaces within the same assay. This fitted value for the initial flux at the surface correlates well with the observed 80% reduction in spore density on Sharklet surfaces during the first 2 h of the assays.

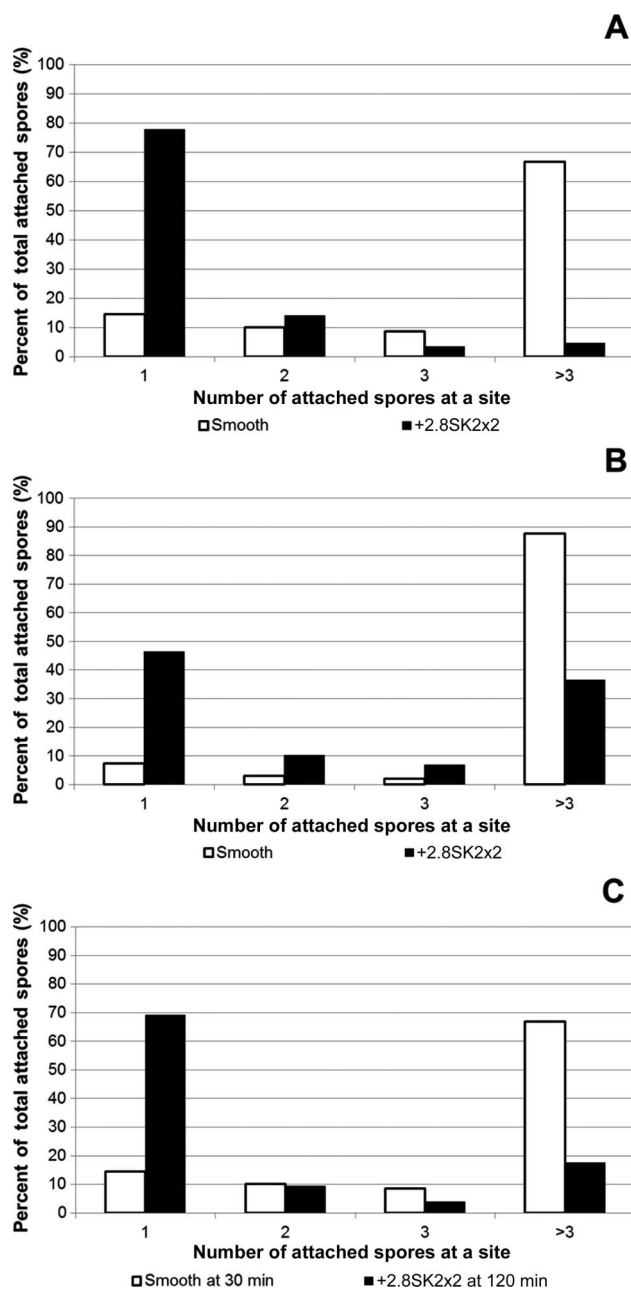


Figure 9. Proportion of spores attached into groups of 1, 2, 3, or > 3 (as determined microscopically by spores touching) at (A) 30 min, (B) 240 min, and (C) a spore density of ~ 200 spores mm^{-2} . A chi-squared test for each condition (A-C) showed that the Sharklet surface has a statistically different distribution from the smooth surface ($p < 0.001$). These samples were taken from the smooth and 6.5 cm^2 Sharklet surface (Figure 1A and B).

The parameter β has been associated with numerous cell-surface phenomena in bacteria including the synthesis of extracellular matrix and the exclusion of bacteria from settling next to neighbors (Dabros and van de Ven 1982; Busscher et al. 1990; van der Mei et al. 1993). While Equation (1) has been effective in

describing adhesion of non-motile bacteria, it was unknown whether this Langmuir-type adsorption process would effectively describe the attachment of motile spores. Indeed, the surface was far from saturated with spores. The surface area coverage was only 6.4% if two assumptions are made, ie the area of an attached spore with its halo of adhesive on PDMSe is $64 \mu\text{m}^2$ (Callow et al. 2005) and the density of spores is 1000 mm^{-2} (maximum on the smooth PDMSe). The assay only captures the response of the zoospores which have strongly committed to adhesion, a process that is fundamentally different to the dynamic adhesion/detachment (or adsorption/desorption) observed for bacterial adhesion. Yet Equation (1) fit with high correlation ($r^2 > 0.9$) and J_o accurately reflected the observed 80% reduction in attachment rate. The lower values for β on the Sharklet topography may reflect a reduced ability for attached spores to cooperatively recruit other spores to the surface. Additional evidence to this end is provided by comparing the grouping of spores on the smooth and Sharklet surfaces.

Spores attach as larger groups on smooth PDMSe (Figure 9). After 45 min, the percentage of spores attached as individuals on smooth PDMSe (contact angle 113°) was 19% (Supplementary Information Figure S4 [Supplementary material is available via a multimedia link on the online article webpage]). This correlated well with a previously published value of $\approx 22\%$ spores attached as singles on flat SAMs with a similar contact angle (110°) after 1 h (Callow et al. 2000). In contrast, a majority of spores (69%) on the Sharklet surface were attached as singles after 45 min (Figure S4). It seems that zoospores were not able to form gregarious communities on the Sharklet pattern. This may simply be due to the fact that the early colonizing spores physically occupy those sites on the Sharklet surface that are topographically the most attractive for attachment (ie a form of 'niche exclusion'). Alternatively, more complex mechanisms may be at work whereby the Sharklet surface inhibited the ability of attached zoospores to recruit neighboring spores to attach. Future quantitative analysis of spore behavior on Sharklet topographies by digital holographic microscopy (Heydt et al. 2007, 2009) may provide further insight into the mechanism(s) involved.

Cooperative behavior has been observed for the attachment of *Ulva* to surfaces (Callow et al. 1997). A Scatchard plot of zoospores binding to glass showed a positive slope at densities $< \sim 1000$ spores mm^{-2} (Callow et al. 1997). This means that at low coverage, the attached cells recruited other cells to the surface. This positively cooperative behavior has also been shown for bacteria binding to surfaces (Krishnamurti and Soman 1951; Sjollem et al. 1990; van der Mei

Table 1. Parameters A_e and β generated by the least squares fit of Equation (1).

Assay	Test area (cm ²)	Surface	A_e (Spores mm ⁻²)	$\beta \times 10^3$ (min ⁻¹)	J_o (Spores mm ⁻² min ⁻¹)	r^2
October 2009	19.4	Smooth	748	9.2	6.9	0.924
	13	Flat Area	639	11	7.0	0.960
	6.5	+2.8SK2 × 2	371	3.4	1.3	0.979
April 2010	19.4	Smooth	1042	11	11.5	0.975
	13	Flat Area	1135	10	11.4	0.963
	6.5	+2.5SK2 × 2	639	2.7	1.7	0.978
	19.4	+2.5SK2 × 2	1046	1.9	2.0	0.988

Note: A_e is the anticipated density of spores at equilibrium ($t \rightarrow \infty$). β is the characteristic time constant and J_o is the flux of spores at the surface.

et al. 1993) and aggregating in suspension (Lin et al. 1995). However, at high densities of attached spores, a different behavior has been observed. The Scatchard analysis showed a negative slope, indicating that the attached spores deterred swimming spores from settling (Callow et al. 1997).

The communication mechanisms underlying the cooperative effects between zoospores of *Ulva* are essentially unknown but may include both diffusible (chemical) cues or physical, topographical cues presented by previously attached spores. It is possible that the inhibitory nature of the Sharklet topography is due to interference in the dynamics of such cooperative effects. For example, the Sharklet topography may simulate a high density of attached spores leading to negative cooperativity, a slower rate of attachment (k_1) and a smaller characteristic time constant (β). While these experiments do not identify the individual rate constants (k_1 and k_{-1}), future experiments such as Scatchard analyses may be able to identify any cooperative behavior on the Sharklet surface.

Acknowledgements

The authors gratefully acknowledge the Office of Naval Research for financial support (contract #N00014-10-1-0579 for support of SPC and ABB and contract #N00014-08-1-0010 for support of JAF, GC, MEC, and JAC). SPC also acknowledges the National Science Foundation Graduate Research Fellowship and the University of Florida Alumni Fellowship for additional funding. The authors would also like to thank Mr Sean Royston for sample preparation. They additionally thank Mr Julian Sheats and Mr Joe Decker for discussions during manuscript preparation.

References

Bressy C, Hellio C, Maréchal JP, Tanguy B, Margailan A. 2010. Bioassays and field immersion tests: a comparison of the antifouling activity of copper-free poly(methacrylic)-based coatings containing tertiary amines and ammonium salt groups. *Biofouling* 26:769–777.

- Busscher HJ, Sjollem J, van der Mei HC. 1990. Relative importance of surface free energy as a measure of hydrophobicity in bacterial adhesion to solid surfaces. In: Doyle RJ, Rosenberg M, editors. *Microbial cell surface hydrophobicity*. Washington (DC): American Society for Microbiology. p. 335–359.
- Callow JA, Callow ME, Ista LK, Lopez G, Chaudhury MK. 2005. The influence of surface energy on the wetting behaviour of the spore adhesive of the marine alga *Ulva linza* (synonym *Enteromorpha linza*). *J R Soc Interface* 2:319–325.
- Callow ME, Callow JA. 2002. Marine biofouling: a sticky problem. *Biologist* 49:10–14.
- Callow ME, Callow JA, Pickett-Heaps JD, Wetherbee R. 1997. Primary adhesion of *Enteromorpha* (Chlorophyta, Ulvales) propagules: quantitative settlement studies and video microscopy. *J Phycol* 33:938–947.
- Callow ME, Callow JA, Ista LK, Coleman SE, Nolasco AC, Lopez GP. 2000. Use of self-assembled monolayers of different wettabilities to study surface selection and primary adhesion processes of green algal (*Enteromorpha*) zoospores. *Appl Environ Microbiol* 66:3249–3254.
- Callow ME, Jennings AR, Brennan AB, Seegert CE, Gibson A, Wilson L, Feinberg A, Baney R, Callow JA. 2002. Microtopographic cues for settlement of zoospores of the green fouling alga *Enteromorpha*. *Biofouling* 18:237–245.
- Carman M, Estes T, Feinberg A, Schumacher J, Wilkerson W, Wilson L, Callow M, Callow J, Brennan A. 2006. Engineered antifouling microtopographies – correlating wettability with cell attachment. *Biofouling* 22:11–21.
- Chung KK, Schumacher JF, Sampson EM, Burne RA, Antonelli PJ, Brennan AB. 2007. Impact of engineered surface microtopography on biofilm formation of *Staphylococcus aureus*. *Biointerphases* 2:89–94.
- Cowan MM, Taylor KG, Doyle RJ. 1986. Kinetic analysis of *Streptococcus sanguis* adhesion to artificial pellicle. *J Dent Res* 65:1278–1283.
- Dabros T, van de Ven TGM. 1982. Kinetics of coating by colloidal particles. *J Colloid Interface Sci* 89:232–244.
- Drake JM, Lodge DM. 2007. Hull fouling is a risk factor for intercontinental species exchange in aquatic ecosystems. *Aquat Invas* 2:121–131.
- Finnie AA, Williams DN. 2010. Paint and coatings technology for the control of marine fouling. In: Durr S, Thomason J, editors. *Biofouling*. Oxford, UK: Wiley-Blackwell. p. 185–206.
- Heydt M, Divós P, Grunze M, Rosenhahn A. 2009. Analysis of holographic microscopy data to quantitatively investigate three-dimensional settlement dynamics of algal zoospores in the vicinity of surfaces. *Eur Phys J E* 30: 141–148.

- Heydt M, Rosenhahn A, Grunze M, Pettitt M, Callow JA, Callow ME. 2007. Digital in-line holography as a three-dimensional tool to study motile marine organisms during their exploration of surfaces. *J Adhesion* 83:417–430.
- Krishnamurti K, Soman S. 1951. Studies in the adsorption of bacteria. *P Indian Acad Sci B* 34:81–91.
- Kristensen JB, Olsen SM, Laursen BS, Kragh KM, Poulsen CH, Besenbacher F, Meyer RL. 2010. Enzymatic generation of hydrogen peroxide shows promising antifouling effect. *Biofouling* 26:141–153.
- Lin L, Rosenberg M, Taylor KG, Doyle RJ. 1995. Kinetic analysis of ammonium sulfate dependent aggregation of bacteria. *Colloids Surf B* 5:127–134.
- Long CJ. 2009. Analytical methods for predicting bio-settlement on patterned surfaces. PhD Dissertation. Gainesville (FL): University of Florida.
- Long CJ, Finlay JA, Callow ME, Callow JA, Brennan AB. 2010a. Engineered antifouling microtopographies: mapping preferential and inhibitory microenvironments for zoospore attachment. *Biofouling* 26:941–952.
- Long CJ, Schumacher JF, Robinson PAC, Finlay JA, Callow ME, Callow JA, Brennan AB. 2010b. A model that predicts the attachment behavior of *Ulva linza* zoospores on surface topography. *Biofouling* 26:411–419.
- Magin CM, Cooper SP, Brennan AB. 2010a. Non-toxic antifouling strategies. *Mater Today* 13:36–44.
- Magin CM, Long CJ, Cooper SP, Ista LK, Lopez GP, Brennan AB. 2010b. Engineered antifouling microtopographies: the role of Reynolds number in a model that predicts attachment of zoospores of *Ulva* and cells of *Cobetia marina*. *Biofouling* 26:719–727.
- McMaster D, Bennett S, Tang Y, Finlay JA, Kowalke GL, Nedved B, Bright FV, Callow ME, Callow JA, Wendt DE, et al. 2009. Antifouling character of ‘active’ hybrid xerogel coatings with sequestered catalysts for the activation of hydrogen peroxide. *Biofouling* 25:21–23.
- Piola RF, Dafforn KA, Johnston EL. 2009. The influence of antifouling practices on marine invasions. *Biofouling* 25:633–644.
- Pratt-Terpstra IH, Weerkamp AH, Busscher HJ. 1988. Microbial factors in a thermodynamic approach of oral streptococcal adhesion to solid substrata. *J Colloid Interface Sci* 129:568–574.
- Scardino AJ, de Nys R. 2011. Mini review: Biomimetic models and bioinspired surfaces for fouling control. *Biofouling* 27:73–86.
- Scardino AJ, Hudleston D, Peng Z, Paul NA, de Nys R. 2009. Biomimetic characterisation of key surface parameters for the development of fouling resistant materials. *Biofouling* 25:83–93.
- Schultz MP, Bendick JA, Holm ER, Hertel WM. 2011. Economic impact of biofouling on a naval surface ship. *Biofouling* 27:87–98.
- Schumacher JF, Long CJ, Callow ME, Finlay JA, Callow JA, Brennan AB. 2008. Engineered nanoforce gradients for inhibition of settlement (attachment) of swimming algal spores. *Langmuir* 24:4931–4937.
- Schumacher JF, Aldred N, Callow ME, Finlay JA, Callow JA, Clare AG, Brennan AB. 2007a. Species-specific engineered antifouling topographies: correlations between the settlement of algal zoospores and barnacle cyprids. *Biofouling* 23:307–317.
- Schumacher JF, Carman ML, Estes TG, Feinberg AW, Wilson LH, Callow ME, Callow JA, Finlay JA, Brennan AB. 2007b. Engineered antifouling microtopographies – effect of feature size, geometry, and roughness on settlement of zoospores of the green alga *Ulva*. *Biofouling* 23:55–62.
- Sjollem J, Busscher HJ, Weerkamp AH. 1989. Experimental approaches to studying adhesion of microorganisms to solid substrata: applications and mass transport. *J Microbiol Methods* 9:79–90.
- Sjollem J, van der Mei HC, Uyen HM, Busscher HJ. 1990. Direct observations of cooperative effects in oral streptococcal adhesion to glass by analysis of the spatial arrangement of adhering bacteria. *FEMS Microbiol Lett* 69:263–270.
- Sommer S, Ekin A, Webster DC, Staflieni SJ, Daniels J, Van der Wal LJ, Thompson SEM, Callow ME, Callow JA. 2010. A preliminary study on the properties and fouling-release performance of siloxane–polyurethane coatings prepared from poly(dimethylsiloxane) (PDMS) macromers. *Biofouling* 26:961–972.
- Tasso M, Pettitt ME, Cordeiro AL, Callow ME, Callow JA, Werner C. 2009. Antifouling potential of Subtilisin A immobilized onto maleic anhydride copolymer thin films. *Biofouling* 25:505–516.
- Thomas KV, Brooks S. 2010. The environmental fate and effects of antifouling paint biocides. *Biofouling* 26:73–88.
- van der Mei HC, Cox SD, Geertsema-Doornbusch GI, Doyle RJ, Busscher HJ. 1993. A critical appraisal of positive cooperativity in oral streptococcal adhesion: scatchard analyses of adhesion data versus analyses of the spatial arrangement of adhering bacteria. *J Gen Microbiol* 139:937–948.